Journal of Molecular Structure, 160 (1987) 1—26
Elsevier Science Publishers B.V., Amsterdam — Printed in The Netherlands

THE VIBRATIONAL SPECTRA, MOLECULAR STRUCTURE AND CONFORMATIONS OF ORGANIC AZIDES

Part V*. 3-Azidopropyne (propargylazide)

J. ALMLÖF, G. O. BRAATHEN, P. KLAEBOE, C. J. NIELSEN** and H. PRIEBE***
Department of Chemistry, University of Oslo, P.O. Box 1033 Blindern, 0315 Oslo 3 (Norway)
S. H. SCHEI
Department of Chemistry, University of Trondheim, AVH N-7055 Dragvoll (Norway)
(Received 13 January 1987)

ABSTRACT

3-Azidopropyne and 3-azidopropyne-1-[^{2}H] have been synthesized; the structure was determined by electron diffraction from the vapour and computed by ab initio Hartree—Fock SCF calculations. IR spectra of the vapour, of the cooled solid, of the matrix isolated species in argon and nitrogen at 13 K, and of the solid at 90 K were recorded. Raman spectra of the cooled liquid and of the amorphous and crystalline solids were also obtained.

From the spectroscopic investigation it is evident that the title compound exists as only one conformer in all states of aggregation. The electron diffraction results and the theoretical calculations show unambiguously the conformation to be *gauche* around the C—N bond with a dihedral angle of 37° (8) from *syn* and with the NNN angle, 169° (4), oriented *anti* to the C—N bond.

The following bond distances (r_a) between the heavy atoms were obtained: $r_{C\equiv C}$ = 121.6(7) pm, r_{C-C} = 148.1(13) pm, r_{C-N} = 146.4(13) pm, $r_{N=N}$ = 124.9(7) pm and $r_{N\equiv N}$ = 113.7(6) pm.

INTRODUCTION

Warning: 3-Azidopropyne is extremely explosive and should be handled with the utmost care. We experienced two violent explosions during the synthesis in which 100 mmol completely ruined a ventilation hood.

The previous papers in this series contain a brief summary of our experimental and theoretical investigations on organic azides [1] and more detailed accounts of the vibrational spectra and the molecular structure of 2-azido-1,3-butadiene [2] and 2,3-diazido-1,3-butadiene [3]. In an ab initio study

*For Part IV of this series see ref. 4.
**Author to whom correspondence should be addressed.
***Present address: NYCOMED, P.O. Box 4220, Torshov, N-0401 Oslo 4, Norway.

0022-2860/87/$03.50

the molecular structures and force fields of hydrazoic acid, azidomethane, azidoethane, azidoethene and azidomethanal [4] were reproted.

3-Azidopropyne (propargylazide, PROPAZ) was synthesized for the first time in 1967 [5]. Together with the synthetic procedure were reported [5] the mass spectrum, the main IR peaks and the ^{1}H NMR chemical shifts and coupling constants. Since then we have published alternative preparations and the spectroscopic data necessary for identification of the compound [6, 7]: we have also given a preliminary report of the UV-photolysis of PROPAZ, isolated in nitrogen matrices at 13 K, monitored by IR spectroscopy [8].

The present paper presents the vibrational spectra and the structure of gaseous PROPAZ as determined by electron diffraction and as calculated by quantum mechanical methods.

EXPERIMENTAL

Preparative

Preparation of the samples of PROPAZ and 3-azidopropyne-1-[^{2}H] (DPROPAZ) has been described elsewhere [6, 7]. For the spectroscopic investigations PROPAZ was prepared from 3-bromopropyne and tetramethylguanidiniumazide in sulfolane [6]. The purity, checked by GC, was better than 98%. The isotopic purity of DPROPAZ was better than 97% judged from the relative intensity of the remaining ≡C—H bands in the IR spectra. Upon standing at —30°C the sample slowly decomposes/polymerizes and among the products formed are ethyne and hydrogen cyanide.

Spectral studies

IR spectra were obtained with a Perkin-Elmer model 225 spectrometer (5000—200 cm^{-1}) and with a Bruker IFS 114C FTIR instrument (4000—20 cm^{-1}). Raman spectra were recorded on a DILOR RTI 30 spectrometer (triple monochromator) interfaced to the Aspect 2000 data system of the Bruker FTIR. The 514.5 nm and 488 nm lines of a CRL 52G argon ion laser were used for excitation.

IR vapour-phase spectra of PROPAZ and DPROPAZ were recorded in cells of path lengths 10 cm (4000—200 cm^{-1}) and 20 cm (650—50 cm^{-1}) equipped with CsI and polyethylene windows, respectively. Spectra of the glassy solid formed by shock freezing the vapour on CsI or silicon windows at ca. 90 K were recorded. The sample was subsequently annealed to 160 K at which temperature the sample turned frosty. After recooling the sample to 90 K, the IR spectra were recorded and they showed it to be crystalline. Spectra of PROPAZ and DPROPAZ isolated in nitrogen matrices (M/A ~1:500) were recorded at ca. 15 K, using a closed cycle cryostat from Air Products. In a moment of distraction we also obtained the IR spectra of PROPAZ as a liquid in a sealed cell cooled to ca. 250 K.

Raman spectra of liquid PROPAZ and DPROPAZ were obtained in a capillary tube of 2 mm inner diameter. The tube was inserted in a transparent Dewar flask [9] and cooled to ca. 210 K by a stream of cold nitrogen. Semiquantitative polarization measurements were carried out. The Raman spectra of the solid samples deposited on a cooled copper block (ca. 90 K) were obtained before and after annealing. It was difficult to obtain a thick polycrystalline sample suitable for Raman scattering as the amorphous solid sample of PROPAZ turned into a transparent "syrup" at ca. 150 K before slowly crystallizing at ca. 160 K. In order to prevent decompositions and possible explosions the laser power was kept well below 100 mW at the sample.

Electron diffraction

The electron diffraction data were recorded on Kodak Electron Image plates with the Balzers Edigraph KDG-2 [10, 11] at a nozzle temperature of 293 K and nozzle-to-plate distances 50 and 25 cm, from which 4 and 5 plates, respectively, were selected for analysis. The electron wavelength was calibrated against benzene [12], optical densities were measured with a Joyce—Loebl densitometer and the data were reduced in the usual way [13, 14] yielding two averaged intensity curves (one from each distance) in the form $sI_m(s)$. Electron scattering amplitudes and phase shifts were calculated employing Hartree—Fock potentials for C and N [15], while molecular bonded potentials were used for H [16].

RESULTS

Vibrational spectra

The IR spectra of gaseous PROPAZ and DPROPAZ are given in Figs. 1 and 2, respectively. Figure 3 shows the IR spectrum of PROPAZ isolated in a nitrogen matrix at ca. 15 K and in Fig. 4 an IR spectrum of DPROPAZ as a crystalline solid at ca. 90 K is given. Finally, a Raman spectrum of PROPAZ as a neat liquid, cooled to ca. 210 K, is shown in Fig. 5. The spectral data for PROPAZ and DPROPAZ are collected in Tables 1 and 2, respectively, and the assigned fundamentals are compared with the results of normal coordinate calculations in Table 3. According to the semiquantitative polarization measurements, all the bands appear to be polarized. Hence, no indication of the depolarization ratios has been included in Tables 1 and 2.

In the synthesis of PROPAZ, tetramethylguanidiniumazide was dissolved in chloroform which was subsequently pumped off under vacuum. However, the very intense IR band at ca. 770 cm^{-1} (vapour) appeared as a weak impurity in some of the spectra. At a conservative estimate the concentration of chloroform in PROPAZ was less than 0.5%. Although the purity of PROPAZ was better than 98%, the strongest bands of the starting material, 3-bromopropyne, also appear as weak impurity peaks in the spectra and, as if these

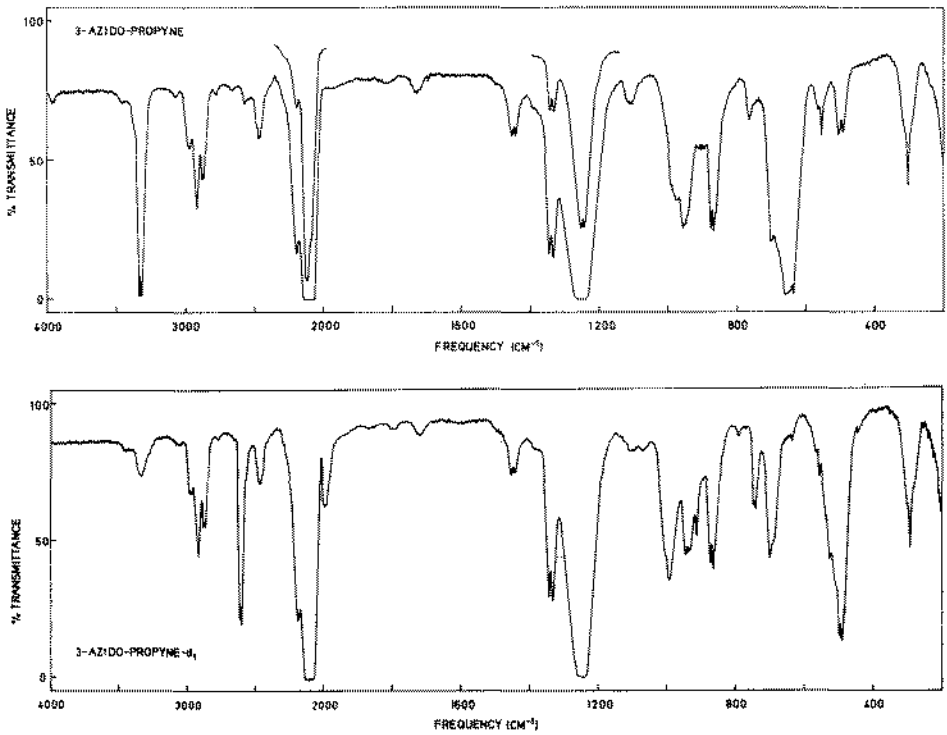

Fig. 1. The mid IR spectrum of 3-azidopropyne as a vapour. Pathlength 10 cm, pressure 30 torr.

Fig. 2. The mid IR spectrum of 3-azidopropyne-1-[^{2}H] as a vapour. Pathlength 10 cm, pressure 30 torr.

impurities were not enough, we also have impurity peaks in the spectra resulting from sample degradation during the recording of the spectra. This is especially true for DPROPAZ for which we only had a small amount of sample available. The bands which are obviously due to impurities have been duly marked in Table 1 and 2.

No significant differences are observed between the gaseous, the liquid and the crystalline phase spectra indicating that only one (or one very dominant) conformer is present in all three phases. The calculated vapour phase band contours for the *anti*, *gauche* and *syn* conformations are shown in Fig. 6. After a quick perusal of the vapour phase spectra (Figs. 1 and 2) and the theoretical vapour-phase band contours in Fig. 6 one can immediately exclude the *anti* conformer as being the dominant form. Unfortunately, it is difficult to distinguish between the band contours corresponding to the *syn* and *gauche* conformations. However, the molecular conformation can be determined from the Raman polarization measurements. As mentioned before,

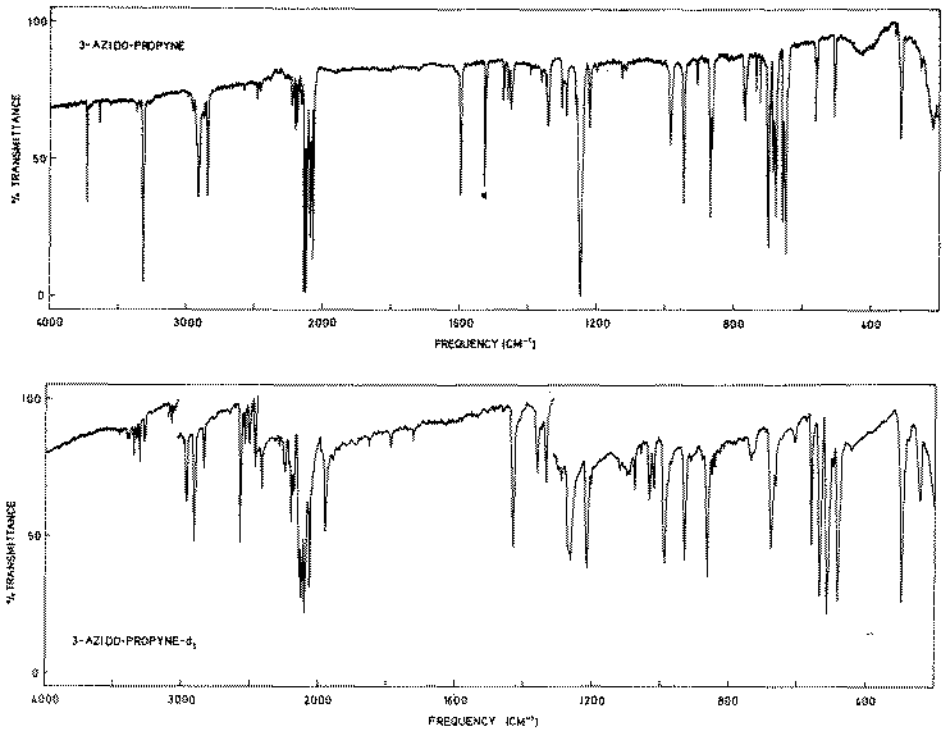

Fig. 3. The mid IR spectrum of 3-azidopropyne trapped in a nitrogen matrix at ca. 15 K (M/A ~ 1:500). The band marked with an asterisk is due to CS_2.

Fig. 4. The mid IR spectrum of 3-azidopropyne-1-[^{2}H] as a crystalline solid at ca. 90 K.

all the bands appear to be polarized, which indicates a *gauche* conformation; only 14 of 21 fundamentals would be expected to be polarized in the *syn* form.

Electron diffraction

The least squares refinements were carried out on the $sI_m(s)$ intensity curves; the composite of the two camera distance curves is shown in Fig. 7: a unit weight matrix was used. The molecular geometry was calculated from the geometry consistent r_α model [17].

Root mean square amplitudes of vibration (l) and perpendicular correction coefficients (K) were constrained to the values calculated from an approximate force field. The set of l- and K-values was adjusted according to the torsional angle and torsional force constant which resulted as the analysis progressed.

A few constraints had to be introduced among the geometrical parameters. The CH_2 group was positioned so that the four CCH and NCH angles were

TABLE 1

Vibrational spectral data[a] for 3-azido-propyne (PROPAZ)

Infrared				Raman			Inter-pretation
Nitrogen matrix 15 K	Vapour	Liquid 250 K	Cryst. solid 90 K	Liquid 250 K	Amorph. solid 90 K	Cryst. solid 90 K	
3364 vw[b]	~3370 w, sh	~3350 m, sh	3361 w 3346 w 3339 w 3319 m				
3313 vs	3338 3331 Q-s, A 3324	3296 vs	3284 vs	3298 m, br	3286 m	3282 m	ν_1
	~3310 m, sh	~3270 s, sh	3266 m	~3260 w, sh	~3250 w		
	~3080 w	~3070 vw		~3065 w	~3065 w		
	~3010 vw	3010 vw			~3010 vw	3011 w	
2980 vw	2991 2985 Q-w, AB 2976	2980 w	2976 ms	2976 m	2974 m	2980 m	ν_2
		2958 vw				2960 w	HCCCH$_2$Br
2930 m	2932 2923 Q-m, AC 2916	2918 m	2921 s	2926 s	2927 s	2924 s	ν_9
						2912 w	
2878 w	2884 2878 Q-m, AB 2872	2862 m	2848 m	2864 m	2862 m	2851 w	$2\nu_6$
2205 m	2211 m, B	2105 m, sh	2218 m	~2200 w			
2190 m	2198		2209 ms				
2165 w	~2150 m, sh		2160 s 2144 vs	~2155 w		~2135 w, sh	
	2135		2136 vs				
2135 vs	2130 Q-vs, AB		2124 s	2125 vs	2122 vs	2122 vs	ν_4
2125 vs	2123	~2110 vs, br	2116 vs	2102 m, sh	2102 w	2108 m	ν_5
2106 m	~2110 s, sh						
2094 s 2087 m	~2090 s, sh		2092 m				
2075 s	~2070 s, sh	2070 s	2078 s	2075 m	2075 w	2076 m	

			2062 m				
	1458						
1450 m	1453 Q—m, A	1442 m	1439 m	1442 m	1441 m	1433 m	ν_6
	1446		1435 s				
		1423 w		1425 vw		1417 vw	$HCCCH_2Br$
1396 vw	~1380 w	~1380 w, sh	1370 m				
1364 w							
1351 w							
	1346						
1341 m	1340 Q—s, AB	1336 m	1340 m	1340 m	1342 m	1343 m	ν_7
	1334						
			1327 w				
			1310 w				
1302 m			1300 w				
1288 m	~1280 m, sh	~1280 m, sh	1281 m	~1265 w, sh		1269 w	
	1256						
1247 vs	1247 Q—s, AB	1250 s, br	1269 vs	1247 m, br	1247 m	1258 m	ν_8
	1241						
	~1230						
1219 m	1218 Q—m, C?	1214 s	1221 s	1214 m	1217 m	1220 m	ν_9
	1208		1217 s				
			1206 w				
1116 vw	~1110 w, B?	1113 w	1121 w	1113 vw			
		1092 w	1094 w	1092 vw			
		1080 w					
		1048 w					
1009 vw			1002 w				
	993						
985 m	981 Q—m, AB	982 m	990 s	984 w	986 w	991 w	ν_{10}
	973		980 s				
				966 w			
		957 m, sh		958 w	957 w	958 w	$HCCCH_2Br$
	956						
945 s	948 Q—m, AB	946 ms	942 s	947 w	944 w	941 m	ν_{11}
	942						
			924 w	920 w	925 w		
	914						
906 w	907 Q—w, C?	903 w	902 w	903 w	902 w		
	894						
			885 w				
	876						
866 s	868 —ms, AB?	862 s	869 vs	861 vs	863 s	870 s	ν_{12}
	862						
			855 w				
			849 w		~850 vw		

TABLE 1 (continued)

Infrared				Raman			Inter-pretation
Nitrogen matrix 15 K	Vapour	Liquid 250 K	Cryst. solid 90 K	Liquid 250 K	Amorph. solid 90 K	Cryst. solid 90 K	
766 w	770 w	755 w	751 mw				$CHCl_3$
	729 Q, w						HCCH
	712 Q, w						HCN
698 s	700 684 — m, B?		686 s	690 m	690 m	684 m	ν_{13}
684 m 676 s 654 s	669 659 652 — vs, B?	~680 vs, br	669 s 666 s	670 m, sh	~655 w, br	~675 w, sh 666 m	ν_{14}
647 s	637 Q — s, C	~650 vs		~650 w, br			ν_{15}
	~625						
				618 w	618 m	620 m	$HCCCH_2Br$
	565						
558 m	558 Q — m, C	554 m	559 s	557 vw	559 vw	561 vw	ν_{16}
	544						
		532 vw	531 vw				
	507						
504 m	501 Q — m, AB	501 m	499 s	503 m	503 m	500 m	ν_{17}
	494						
				425 vw			$H_2CCCHBr$
		395 vw	~400 vw	398 w	400 m	400 w	$HCCCH_2Br$
				366 vw			$CHCl_3$
	315						
311 m	304 Q — m, C	310 ms	310 vs	313 s	316 s	319 s	ν_{18}
	295						
253 w	~245 w	~250 w, br	258 s	256 s	258 s	247 s	ν_{19}
	172						
	160 Q — w, AB	188 m, br[c]	212 m	~180 w, br	176 m, br	204 s	ν_{20}
	152						
						124 s	
		~110 w, br[c]	102 m 82 m	~70 w, br		102 s	ν_{21}?

[a]Weak bands in the regions 5000—3400, 2800—2300 and 2000—1500 cm^{-1} are omitted. [b]Abbreviations: w, weak; m, medium; s, strong; v, very; br, broad. [c]Frequencies from the amorphous solid at 90 K.

TABLE 2

Vibrational spectral data[a] for 3-azidopropyne-1-[^{2}H] (DPROPAZ)

Infrared				Raman			Inter-pretation
Nitrogen matrix 15 K	Vapour	Amorph. solid 90 K	Cryst. solid 90 K	Liquid 250 K	Amorph. solid 90 K	Cryst. solid 90 K	
	~2980 w[b]	2980 w	2983 w 2974 w	2976 m	2978 m	2983 m 2975 m	ν_1
2930 w	2930 2921 Q 2915 — m, AB	2921 w	2923 w	2924 s	2926 s	2924 s	ν_2
2881 vw	2882 2876 Q 2870 — w, AB	2859 w	2852 w	2863 mw	2860 w	2853 w	$2\nu_6$
2602 vs	2618 2611 Q 2604 — s, AB	2586 s	2584 s	2590 w	~2575 w	2584 w	ν_3
2593 w		2568 s					
		2201 m	2213 m				
2183 w		2182 m	2192 m				
2157 w		~2150 s, sh	2151 s				
2153 w							
2128 vs	2135 2123 — vs	2130 vs	2139 vs 2134 vs	2121 m	2126 mw	2109 m	ν_4
2100 w				2101 w	2101 w		
2092 s	~2090 s, sh	2105 vs	2114 vs				
2074 s	~2070 s, sh	2070 s	2076 s	2070 w	2071 w	2075 mw	
1996 w	2005 1992 — w, B	1997 m	1997 m	1985 vs	1985 vs	1984 vs	ν_5
				~1950 w	1976 s, sh	1964 w	
				1924 w	1926 w	1923 w	
1451 w	1458 1452 Q 1446 — w, AB	1439 m	1435 m	1440 m	1441 m	1435 m	ν_6

TABLE 2 (continued)

Infrared				Raman			Inter-pretation
Nitrogen matrix 15 K	Vapour	Amorph. solid 90 K	Cryst. solid 90 K	Liquid 250 K	Amorph. solid 90 K	Cryst. solid 90 K	
				~1415 vw			
	~1380 vw		1366 m				
1343 w	1344						
1340 w	1332 m, B	1339 m	1339 m	1338 m	1340 m	1342 m	ν_7
			~1280 m, sh	~1285 w, br			
	1257						
1248 vs	1249 Q vs, AB	1248 vs	1266 vs	1243 m	1246 m	1268 w 1258 m	ν_8
	1244						
1220 w		1214 ms	1219 m 1217 m	1212 m	1216 m	1221 m	ν_9
	~1105 vw		1119 w				
	~1070 vw		1093 w				
1017 w							
	1007		1023 w, br	1027 vw			
1011 w	994 m		994 m	1001 vw			
984 w	994 m	985 m	991 m	~980 w, br	~985 w, br	994 w	ν_{10}
976 w	982		981 w				
			972 w				
	946		941 vw				
936 m	938 Q m, AB	935 ms	934 ms	933 w	935 mw	933 mw	ν_{11}
	932		928 w, sh				
	913 Q, m	914 w	914 vw	~915 vw			
		904 w					
	873						
863 s	865 s	863 s	865 s	858 s	863 s	867 s	ν_{12}
	859		852 w				
			844 w				
				838 w	837 w	827 w	
	794 vw		~790 vw	~785 w			
	744 m	737 m					impurity
	729 Q, m	731 m					HCCH
	712 Q, m	709 m, sh					HCN

695 s	699 688 — m, B	694 s	681 ms	692 m, br	696 mw	683 m	ν_{13}
			668 w				parent
	637 Q, w	649 vw					parent
		628 vw					
		612 vw	612 vw				
		608 vw	608 vw				
			577 vw	575 w	579 w	~575 w	
	566						
560 m	558 Q — m, C	558 ms	562 ms	~560 w, sh	~560 w, sh	~560 vw	ν_{14}
543 m	~545						
540 m	537 Q — m	544 ms	539 ms	540 m	544 m	540 m	ν_{15}
	526						
515 m	512						
510 m	499 Q — s, C	510 s	517 s	507 m	511 m	517 m	ν_{16}
507 m	492		512 m, sh				
492 m	484 Q — s	491 s	486 s	489 m	494 m	487 mw	ν_{17}
	~475						
				386 m	389 mw	383 w	impurity
	304						
	293 Q — m, C	306 s	300 s	301 s	306 m	310 m	ν_{18}
	281						
		251 w	245 w	249 s	253 ms	245 m 240 m	ν_{19}
		183 w, br	204 m	~170 m	~170 m, br	198 m	ν_{20}

[a]Weak bands in the regions 5000—3000, 2800—2300 and 1900—1500 cm^{-1} are omitted. [b]Abbreviations: w, weak; m, medium; s, strong; v, very; br. broad.

TABLE 3

Observed and calculated fundamental modes of vibration [cm^{-1}] for 3-azidopropyne (PROPAZ) and 3-azidopropyne-1-[^2H] (DPROPAZ)

No.	PROPAZ		DPROPAZ		Description
	Obs.	Calc.[a]	Obs.	Calc.[a]	
ν_1	3331	3343	2611	2597	≡C—H(D) stretch
ν_2	2985	3023	2980	3023	a. sym. CH_2 stretch
ν_3	2923	2919	2921	2919	sym. CH_2 stretch
ν_4	2130	2104	2129	2104	N≡N stretch
ν_5	2110	2122	1999	1984	C≡C stretch
ν_6	1453	1438	1452	1438	CH_2 bend
ν_7	1340	1336	1338	1336	N=N stretch
ν_8	1247	1253	1249	1253	CH_2 wag
ν_9	1218	1224	1220	1224	CH_2 twist
ν_{10}	981	1001	985	994	C—C stretch
ν_{11}	948	934	938	933	CH_2 rock
ν_{12}	868	857	865	853	C—N stretch
ν_{13}	692	701	692	698	NNN bip
ν_{14}	669	645	537	501	C≡C—H(D) bend
ν_{15}	637	642	499	495	C≡C—H(D) bend
ν_{16}	558	556	558	556	NNN bop
ν_{17}	501	486	484	476	C—C—N bend
ν_{18}	304	307	293	300	C—C≡C bend
ν_{19}	245	258	249	252	C—C≡C bend
ν_{20}	160	142		139	C—N=N bend
ν_{21}		58		57	C—N torsion

[a]The force field is listed in Table 10.

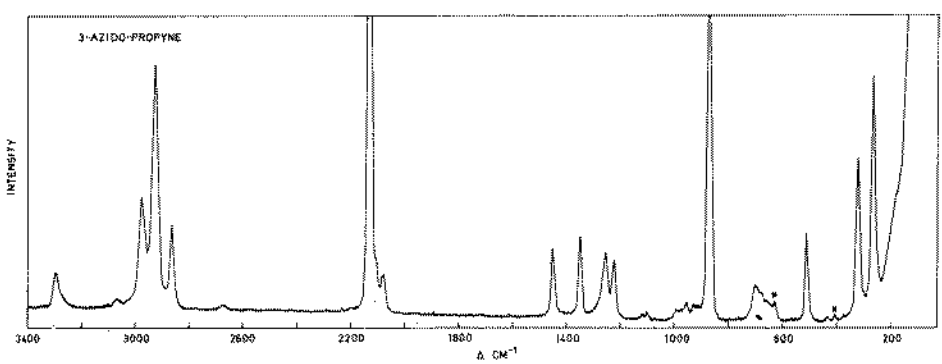

Fig. 5. Raman spectrum of 3-azidopropyne as a liquid at ca. 210 K. The weak bands marked with asterisks are due to 3-bromopropyne.

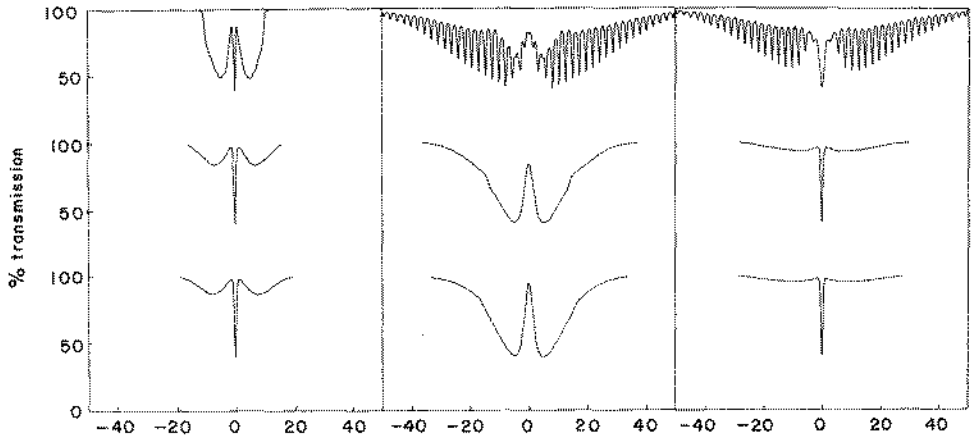

Fig. 6. Calculated IR vapour phase band contours for the *anti* (top), *gauche* (middle) and *syn* (bottom) conformation of 3-azidopropyne.

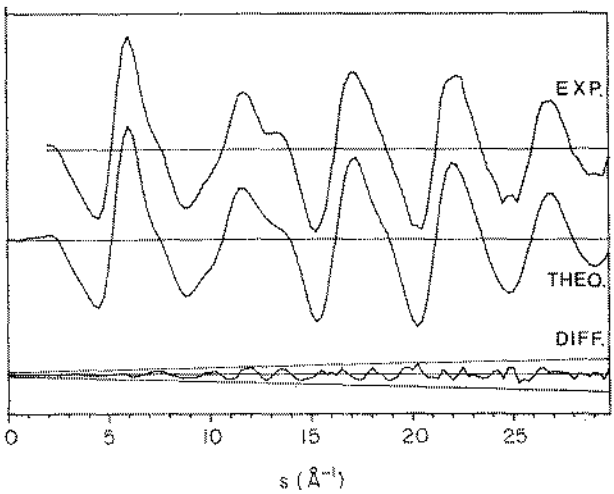

Fig. 7. 3-Azidopropyne intensity curves in the form $sI_m(s)$. Experimental curve is the composite of all plates and camera distances. Theoretical curve was calculated from parameters in Tables 4 and 5. All curves are on the same scale. The straight lines give the experimental uncertainty as three times the standard deviation. $\Delta s = 0.25$ Å^{-1}.

equal. The difference between the two types of C—H distance was kept at the ab initio calculated value of 2.7 pm. The CCC fragment was assumed linear and there was no detectable deviation from the calculated shrinkage. By systematic testing, the bending of the NNN fragment was found to be *anti* relative to the CNN angle.

The electron diffraction data clearly indicated a large torsional movement. However, the form of the torsional potential function could not be accurately

determined from the experimental data, and the torsional motion was hence approximated to by a gaussian function described by six pseudo conformers at 20° intervals. This led to a minimum at a dihedral angle $\theta_0 = 37(8)^\circ$ from *syn*. Further, the root mean square torsional amplitude was found to be $\langle(\theta - \theta_0)^2\rangle^{1/2} = 27(7)^\circ$, which, in the harmonic approximation [18], is associated with a torsional force constant $F_8 = 0.02$ mdyn Å rad^{-2}, giving a torsional frequency of 32 cm^{-1}.

The calculated vibrational amplitudes corresponding to $\theta_0 = 37^\circ$ are listed in Table 4, including those used in the single conformer model ($F_8 = 0.02$ mdyn Å rad^{-2}) and those which were used in the gaussian model.

TABLE 4

3-Azidopropyne (PROPAZ), interatomic distances (r)[a] and calculated root mean square amplitudes of vibration (l) in pm

Distance	r_a	$l \times 10$	
		A[b]	B
$\equiv C_2—H_1$	108	74	
$C_4—H_5$	111	78	
$N_8—N_9$	114	34	
$C_2 \equiv C_3$	122	36	
$N_7—N_8$	125	40	
$N_7—C_4$	146	50	
$C_3—C_4$	148	46	
$C_3 \cdots H_5$	202	106	
$N_7 \cdots H_5$	202	104	
$N_8 \cdots C_4$	226	71	
$C_9 \cdots H_1$	228	79	
$N_7 \cdots N_9$	237	44	
$N_7 \cdots C_3$	246	82	
$N_8 \cdots C_3$	249	249	98
$N_8 \cdots H_5$	267	318	160
$C_2 \cdots C_4$	269	51	
$N_8 \cdots H_6$	293	144	103
$N_9 \cdots C_4$	332	95	
$N_9 \cdots C_3$	335	376	123
$N_8 \cdots C_2$	339	346	124
$N_7 \cdots C_2$	354	108	
$N_9 \cdots H_5$	364	449	209
$C_4 \cdots H_1$	375	86	
$N_9 \cdots C_2$	383	584	142
$N_9 \cdots H_6$	398	182	108
$N_8 \cdots H_1$	422	408	186
$N_9 \cdots H_1$	447	710	221
$N_7 \cdots H_1$	453	151	

[a] Distances correspond to a torsional angle of 37°. Atomic numbering given in Fig. 8.
[b] A: torsional force constant 0.02 mydn Å rad^{-2}, B: contribution from torsional motion excluded.

The agreement between the experimental intensity curve and the theoretical curve was not improved by direct use of the torsional distribution obtained from the ab initio calculations. However, an unsymmetrical potential function was indicated by $\langle\theta\rangle = 45(6)^\circ$ when only one conformer was used to represent the torsional movement.

The experimental results for the C—C and C—N distances were quite uncertain, and the difference between them exhibited an opposite trend to those from the ab initio calculation. Therefore, the electron diffraction data were also analyzed under the assumption that $r_{C-N} - r_{C-C} = 4.6$ pm, the ab initio value. The result from that refinement is included in Table 5 together with the result from the refinement with unconstrained r_{C-N} and r_{C-C}. The radial distribution curve corresponding to the less constrained model is shown in Fig. 8 together with the experimental curve. There are a few large correlation coefficients among the geometry parameters. Those larger than 0.5 have been included in Table 5.

TABLE 5

3-Azidopropyne (PROPAZ), final results from the least squares refinements of the electron diffraction data[a] at 20° C and ab initio calculated results

No.	Parameter	$r_a/\angle_\alpha$		Ab initio r_e
		A	B	
1	r(C≡C)	121.6(7)	122.6(10)	119.1
2	r(C—C)	148.1(13)	144.9(5)	146.6
3	r(C—N)	146.4(13)	149.5	151.2
4	r((C)N—N)	124.9(7)	124.1(9)	125.7
5	r(N)N—N)	113.7(6)	113.7(5)	111.1
6	r(—C—H)	111.1(46)	110.5(43)	108.3
7	r(≡C—H)[b]	108.4	107.8	105.6
8	∠C—C—N	114.6(2)	113.7(13)	115.2
9	∠C—N—N	114.5(15)	112.4(16)	114.8
10	∠N—N—N[c]	169.2(41)	171.2(43)	172.6
11	⟨∠C—C—H⟩ ⟨∠N—C—H⟩	107.6(31)	107.4(33)	110.3
12	θ_0	37(8)[e]	46(7)	39[e]
13	$\langle(\theta-\theta_0)^2\rangle^{1/2}$	27(8)[e]	20(5)	32[f]
	R[d]	6.1/8.7	8.7/9.5	

Correlation coefficients > 0.5:

$C_{1,4} = -0.65$; $C_{2,3} = -0.84$; $C_{5,6} = -0.69$; $C_{6,11} = -0.58$
$C_{8,9} = 0.52$; $C_{8,12} = -0.63$; $C_{9,10} = 0.65$; $C_{9,12} = -0.60$
$C_{12,13} = -0.77$

[a] A: results when r(C—N) and r(C—C) are unconstrained, B: results when r(C—N) — r(C—C) was constrained to the ab initio calculated value. [b] Constrained relative to r(—C—H) as given by the ab initio results. [c] Bent *anti* relative to the CCN angle. [d] R-factors for long and short camera data, respectively. [e] The electron diffraction results are based on a gaussian distribution for the torsional motion, while the ab initio values correspond to the unsymmetrical distribution in Fig. 10. [f] $\langle(\theta - \langle\theta\rangle)^2\rangle^{1/2}$.

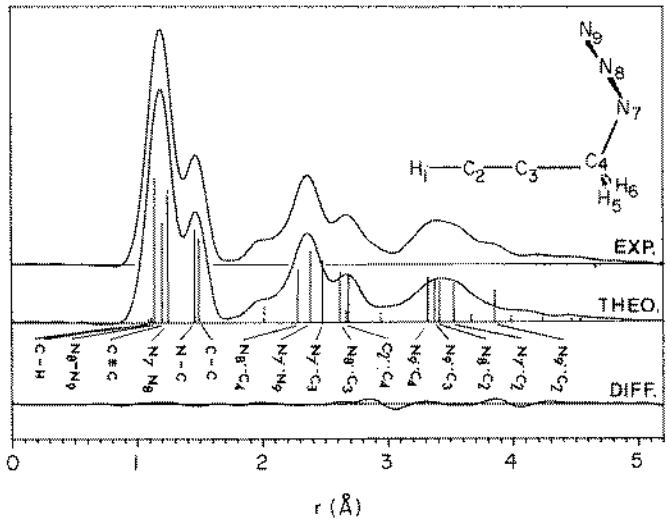

Fig. 8. 3-Azidopropyne, radial distribution curves calculated from the intensity curves in Fig. 7 after multiplication by $(f_N(s)f_C(s))^{-1}$, using theoretical data for unobserved area $s < 2.0$ Å^{-1} and a damping factor $B = 0.002$ Å^2. Dotted vertical lines show N··H distances. All curves are on the same scale.

Quantum mechanical calculations

The experimental investigations indicate that the potential for the torsional vibration around the C—N bond is rather shallow and that the molecular structure is not accurately described by a static model alone. It would therefore be a valuable exercise to illuminate this subject from a theoretical viewpoint. Furthermore, since the C—N and C—C single bond distances are nearly equal, their determination in an ED study would benefit from a comparison with a reliable theoretical geometry. Accordingly, ab initio Hartree—Fock calculations have been performed in order to investigate the molecular structure, and the barrier to internal rotation, further. The torsional angle was kept fixed at intervals of 60°, and all the other internal degrees of freedom were relaxed. In addition, a total optimization has been performed without any restrictions on the geometry. All the calculations were done with a gradient version of the program MOLECULE [19, 20]. A basis set of double-zeta quality has been used, contracted from 7*s*3*p* primitive sets for C and N [21], and from a 3*s* set for H [22]. The relaxation of the geometry was continued until all Cartesian forces on the atoms were less than 0.0001 atomic units.

The global geometry optimization resulted in an energy minimum for a dihedral angle around the C—N bond of 38.8° from *syn*. The calculated total energies are given in Table 6 for the different geometries considered. In Fig. 9 the bond distances and angles for the *syn*, *anti* and *gauche* (minimum energy) conformations are shown.

TABLE 6

Ab initio calculated total energies at different torsional angles for 3-azidopropyne (PROPAZ)

Angle	E_{tot} [hartree]	E_{rel} [kJ mol^{-1}]
0.0 (*syn*)	−278.14450	6.56
38.8 (*min*)	−278.14700	0
60.0	−278.14672	0.74
120.0	−278.14492	5.46
180.0 (*anti*)	−278.14374	8.56

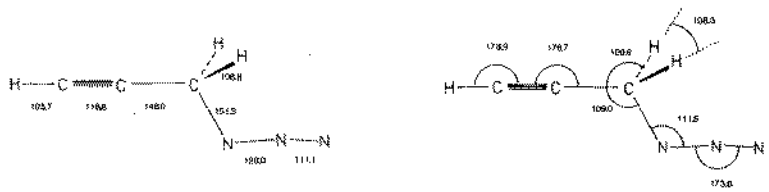

ANTI

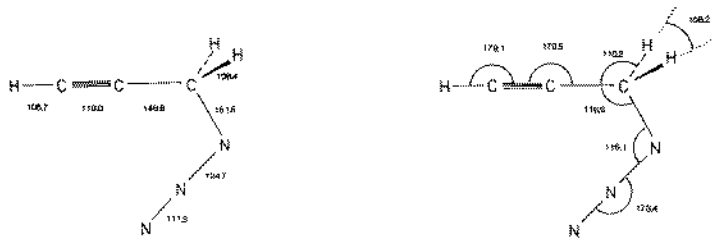

SYN

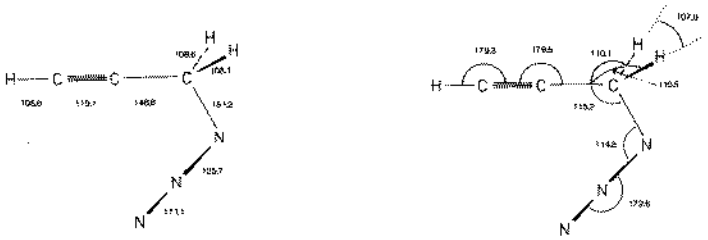

GAUCHE

Fig. 9. The ab initio calculated bond distances (pm) and angles for the *syn*, *gauche* and *anti* conformations of 3-azidopropyne.

In order to study the internal rotation in more detail, an analytic representation of the torsional potential is required. A Fourier series was therefore fitted to the computed energies, with the additional requirement of a minimum at 38.8°, and maxima at 0° and 180°. It was soon found, however, that a better fit could be obtained with other types of functions, the one finally used being of the form

$$V(\theta) = 4.715 \times 10^{-7} \exp\{16.6 \cos(\theta)\} + 12.74 \exp\{-0.38 \cos(\theta)\} \times [\text{kJ mol}^{-1}]$$

Using this potential, torsional frequencies were computed within a rigid-framework assumption. The reduced moment of inertia used in these calculations was obtained from the minimum-energy structure. The wavefunctions were expanded in a series of rigid-rotator eigenstates:

$$f_{i+} = C_{ik+} \cos(k\theta)$$

$$f_{i-} = C_{ik-} \sin(k\theta)$$

In our calculations, expansions with $n = 100$ were used, giving convergence to better than 0.01 cm^{-1} for the 40—50 lowest states. Due to the two-fold symmetry of the potential, the even (cos) and odd (sin) states are separated. The barriers at 0° and 180° are high enough to practically eliminate the interaction between the lower lying states, which are localized in the potential wells at ±38.8°. These states are therefore doubly degenerate for all practical purposes (as opposed to the situation in a free rotator, this degeneracy occurs also in the ground state). Figure 10 shows the torsional potential and the eight lowest torsional levels.

Since the torsional potential is quite anharmonic, the minimum at 38.8° cannot be directly compared with the ED experiment. This is illustrated by the average values $\langle\theta\rangle$ and $\langle(\theta - \langle\theta\rangle)^2\rangle^{1/2}$ shown in Table 7 for some of the lower states. Due to the low frequency of the torsional vibration, a substantial number of the molecules are in torsionally excited states at room temperature. In Table 8 the Boltzmann averages of the angle θ and the variance are given for a selection of different temperatures.

DISCUSSION

Structure

The present theoretical treatment of internal rotation is clearly an approximate one from several points of view. The torsional potential, calculated at the Hartree—Fock level of approximation, is probably accurate within 1—1.5 kJ/mol. The approximation involved in the analytic representation of the potential is likely to be much smaller. Our one-dimensional model for the torsional vibrations, neglecting coupling with the framework vibrations as well as with the external rotation, gives rise to further errors. However, for

TABLE 7

Average values of the torsional angle, θ, and variances $\langle(\theta - \langle\theta\rangle)^2\rangle^{1/2}$ for some of the lower torsional states of 3-azidopropyne (PROPAZ)

State	$\langle\theta\rangle$[a]	$\langle(\theta - \langle\theta\rangle)^2\rangle^{1/2}$
0	39.7	5.9
1	43.1	10.4
2	46.2	13.6
3	49.1	16.3
4	51.7	18.7
5	54.2	20.9
6	56.5	23.0
7	58.7	24.9
8	60.8	26.7
9	62.8	28.6
.	.	.
.	.	.
.	.	.
.	.	.
.	.	.
.	.	.
14	71.5	35.9

[a]Calculated using the theoretical torsional potential shown in Fig. 10.

TABLE 8

Boltzmann averages of the torsional angle, θ, and the variance, $\langle(\theta - \langle\theta\rangle)^2\rangle^{1/2}$, at different temperatures

T [K]	$\langle\theta\rangle$[a]	$\langle(\theta - \langle\theta\rangle)^2\rangle^{1/2}$
0	39.7	5.9
100	44.7	14.3
200	51.2	24.2
300	57.5	32.0
400	62.8	37.5
500	66.8	40.9

[a]Calculated using the theoretical torsional potential shown in Fig. 10.

the purpose of estimating the magnitude of the vibrational correction to the effective equilibrium torsional angle, the approach used here should be adequate. It is not entirely fortuitous that the angle calculated from the Bolttzmann distribution at 300 K agrees fairly well with the experiments, and indeed much better than the potential minimum θ_e.

Concerning the geometrical parameters, Table 5 shows good agreement between the ab initio calculated structure and the experimentally obtained parameters except for the C—C and C—N distances. In fact, for the angle

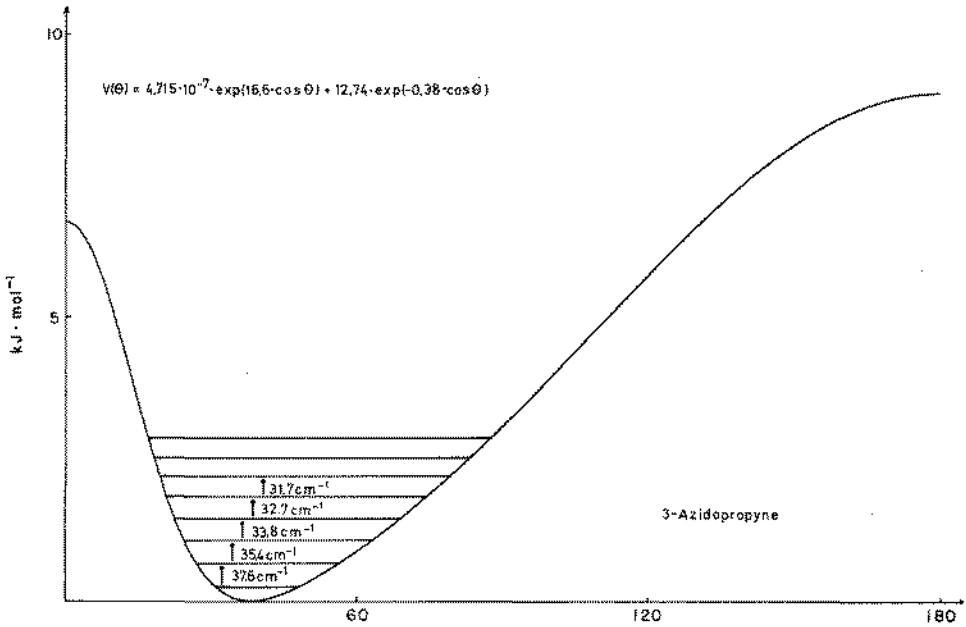

Fig. 10. The approximate torsional potential for 3-azidopropyne from ab initio Hartree—Fock SCF calculations.

parameters the agreement is better when these distances are refined unconstrained than when kept at the calculated difference. Unfortunately, the relative values of these two distances have a noticeable influence upon some of the other parameters. It should be noted that the r_{C-C} came out larger than r_{C-N} in all refinements based on the electron diffraction data, regardless of whether one single conformer or a symmetric or unsymmetric torsional potential with several pseudo conformers were used.

Although it was not possible to determine the asymmetry in the vicinity of the energy minimum from the electron diffraction data, the results with respect to the position of minimum energy and the width of the torsional potential agree well with the calculated results.

The experimental structural results for PROPAZ are compared with the geometry of related molecules in Table 9, which shows that the PROPAZ geometry is largely as expected. The bending of the NNN fragment was clearly revealed by the experimental data and fits well with the trend indicated for several other azides by MNDO calculations [23] and by the more elaborate Hartree—Fock SCF calculations [4].

Spectral interpretation

As a starting point in assigning the vibrational spectra of PROPAZ one can consider the molecule as a fusion of methylazide and a 3-substituted propyne.

TABLE 9

Comparison of some of the geometrical parameters [pm, deg.] of 3-azidopropyne with related molecules

Molecule	$r_{C\equiv C}$	$r_{\equiv C-C}$	$\angle CCX$	r_{C-N}	$r_{N=N}$	$r_{N\equiv N}$	$\angle CNN$	$\angle NNN$	Ref.
$HC\equiv C-CH_3$[a]	120.7(5)	145.8(5)							40
$HC\equiv C-CH_2Cl$[a]	120.7[b]	146.5(20)	111.5(20)						41
$HC\equiv C-CH_2Br$[a]	120.7[b]	145.5(20)	112.0(20)						42
$HC\equiv C-CH_2CH_2-C\equiv CH$	122.0(1)	145.9(1)	110.7(3)						43
$HC\equiv C-CH_2CH_2-C\equiv CBr$	121.7(5)	146.5(6)	110.7(3)						44
$BrC\equiv C-CH_2CH_2-C\equiv CBr$	121.9(2)	146.9(3)	111.9(9)						45
$HC\equiv C-CH_2-N=N\equiv N$	121.6(7)	148.1(13)	114.6(12)	146.4(13)	124.9(7)	113.7(6)	114.5(15)	169.2(41)	This work
$N\equiv C-CH_2-N=N\equiv N$		146.5(15)	113.4(10)	147.6(6)	124.5(5)	113.5(4)	115.4(11)	173(3)	29
$CH_3C\equiv C-CH_2-N=N\equiv N$	120.8(6)	146.8(5)	113.8(16)	147.4(15)	124.0(6)	114.2(5)	116.5(14)	174(5)	30
$H-N=N\equiv N$					124.3(5)	113.4(2)		171.3(50)	46
$CH_3-N=N\equiv N$				146.8(5)	121.6(4)	113.0(5)	116.8(3)	180[b]	47
$CF_3-N=N\equiv N$				142.7(5)	125.0(7)	111.7(4)		175.3(43)	48
$N\equiv C-N=N\equiv N$				135.5(2)	126.1(1)	112.7(2)	114.5(2)	169.2(16)	49
$CH_2-O-CH_2-C-(CH_2N_3)_2$			111.4(12)	147.0(9)	124.0[c]	114.2	119.2(10)	180[b]	50

[a] r_0 structure. [b] Assumed. [c] Given as $NH_{avg.} = 1.191(2)$ and $NN_{diff.} = 0.098(2)$.

The azido group is often considered as a pseudo halogen and accordingly the spectra of PROPAZ display many similarities with the spectra of both methylazide [24—26] and the 3-halopropynes [27, 28]. However, a few comments on the assignment are appropriate.

Spectral similarities with other related compounds are always important factors to consider during spectral interpretation. In addition to the spectra of the 1-[^{2}H] isotopic substituted molecule, which give valuable information in the C≡C stretching and C≡C—H(D) bending regions, we also have the spectral data from the isoelectronic compound azidoacetonitrile [29] and from azido-2-butyne [30] which will be presented in subsequent papers.

The C≡C and N≡N (or the antisymmetric NNN) stretching modes are, accidentally, nearly degenerate in PROPAZ and the spectra are complex around 2100 cm^{-1} with many combination bands or overtones in Fermi resonance with the fundamentals. The C≡C stretching mode normally appears with a weak-to-medium intensity in the IR and as a very strong band in the Raman effect: for the N≡N stretching mode the situation is the reverse. In PROPAZ it is difficult to make an unambiguous assignment of these fundamentals, but in DPROPAZ the C≡C stretching mode is shifted towards lower wavenumbers, the degeneracy lifted and the two fundamentals easily recognized as 2129 and 1999 cm^{-1} for the N≡N and C≡C(D) stretchings, respectively.

In the 3-halopropynes [27, 28] the CH_2 wagging mode causes one of the strongest IR bands with a corresponding Raman band of medium intensity. In PROPAZ and DPROPAZ the CH_2 wagging mode has been assigned to the strong IR bands around 1250 cm^{-1}, with medium intensity Raman counterparts flanked by the N=N stretching mode at ca. 1340 cm^{-1} and the CH_2 twisting mode at ca. 1215 cm^{-1}. However, according to the normal coordinate analysis (NCA) the local mode description of these three fundamentals is inadequate. This is also reflected by the rather high IR intensity of the CH_2 twisting mode. Finally, the CH_2 rocking mode has been assigned to the bands at ca. 950 cm^{-1}. In DPROPAZ the CH_2 rocking mode is, quite unexpectedly, shifted ca. ten wavenumbers downwards. This might be explained by Fermi resonance involving overtones of the C≡C—D bending vibrations.

The C—C and C—N stretching vibrations have been assigned to the bands around 980 and 870 cm^{-1}, respectively, as compared to 940—960 cm^{-1} for the C—C stretching in the 3-halopropynes [27, 28] and ca. 910 cm^{-1} for the C—N stretching in methylazide [24, 25, 26]. According to the NCA it is better to describe ν_{10} (981 cm^{-1}) as the antisymmetric and ν_{11} (868 cm^{-1}) as the symmetric C—C/C—N stretching vibrations. This is also in agreement with the frequency shifts relative to the more localized normal vibrations of the molecular building units. In DPROPAZ the antisymmetric C—C/C—N stretching mode, ν_{12}, is somewhat obscured in the IR spectrum by the overtones of the C≡C—D bending vibrations, but in the Raman effect these are very weak and ν_{12} appears with the same intensity and approximately the same frequency as in PROPAZ.

The in-plane and out-of-plane bending modes of the NNN group (or rather, the NNN bending and the N=N torsional mode) have been assigned to the bands around 690 and 550 cm^{-1}, respectively. Both bands are virtually unaffected by substitution of the acetylenic hydrogen, and the low intensity in the Raman effect [1] is characteristic of the N=N torsional model.

The assignment of the C≡C—H(D) bending modes hardly need any comments, though it is worth noticing the rather large splitting (30 cm^{-1}) between the in-plane and out-of-plane modes.

Of the remaining five modes the C≡C—C bip and bop with respect to the C≡C—C—N plane, the C—C—N and C—N=N bendings and the C—N torsional mode) only the C≡C—C bop is characteristic and has accordingly been assigned to the *C*-type band around 300 cm^{-1}, close to the similar a''-mode in the 3-halopropynes [27, 28]. We tentatively assign the weak, broad band around 70 cm^{-1} in the Raman spectra of the cooled liquid to the C—N torsional mode but this is quite uncertain. The description of the last three bending modes ν_{17}, ν_{19} and ν_{20} at ca. 500, 250 and 160 cm^{-1} relies upon the normal coordinate claculations which indicate a strong mixing of the local modes C≡C—C bip and the C—C—N and C—N=N bendings. The main contributors to the potential energy distribution are included in Table 3.

Force constant calculations

Approximate, local symmetry force fields (LSFF) for PROPAZ, azidoacetonitrile and azido-2-butyne were constructed from a scaled quantum mechanical (SQM) force field for the *gauche* conformation of ethylazide [4] and from a LSFF for the 3-halopropynes, the haloacetonitriles and the halo-2-butynes. The latter force fields were derived by the overlay technique using dimensionless stretching coordinates, $\Delta r/r_e$, and constraining the C—halogen stretch and stretch/bend force constants to be the same for the different halogenated compounds. This approximation has proved very useful in the cases of the halogenated malononitriles [31], the monohalogenated cyclohexanes, the *trans*-1,4-dihalocyclohexanes [32, 33] and the halogenated neopentanes [34—36]. The vibrational frequencies used for calculating the force field were taken from the literature [27, 28, 37—39].

The definition of the internal symmetry coordinates is given in Table 10 which also contains the corresponding force field. Only minor adjustments of the CH_2 rock and wag force constants and of the N=N torsional force constant were necessary in order to obtain a reasonably good agreement with the observations for the above mentioned azides as illustrated for PROPAZ and DPROPAZ in Table 3. It must be emphasized that the rest of the force constants have not been modified from their transferred values. The corresponding results for azidoacetonitrile and azido-2-butyne will be given in subsequent papers [29, 30].

TABLE 10

Definition of internal, local symmetry coordinates and local symmetry force field (LSFF)[a]

$S_1 = \Delta r_{89}$ $S_2 = \Delta r_{78}$ $S_3 = \Delta r_{47}$ $S_4 = \Delta r_{34}$ $S_5 = 2^{-1/2}(\Delta r_{45} + \Delta r_{46})$
$S_9 = 1/2(\Delta\alpha_{746} + \Delta\alpha_{745} + \Delta\alpha_{346} + \Delta\alpha_{345})$ $S_{10} = 1/2(\Delta\alpha_{746} + \Delta\alpha_{745} - \Delta\alpha_{346} - \Delta\alpha_{345})$
$S_{12} = 1/2(\Delta\alpha_{746} - \Delta\alpha_{745} + \Delta\alpha_{346} - \Delta\alpha_{345})$ $S_{13} = 1/2(\Delta\alpha_{746} - \Delta\alpha_{745} - \Delta\alpha_{346} + \Delta\alpha_{345})$
$S_{14} = \Delta\tau_{4789}$ $S_{15} = \Delta\tau_{3478}$ $S_{16} = \Delta r_{12}$ $S_{17} = \Delta r_{23}$ $S_{18} = \Delta\theta_{123}(\parallel)$[b] $S_{19} = \Delta\theta_{123}(\perp)$

17.115									
1.799	9.484								
—0.152	0.228	4.275							
0.031	—0.018	0.258	5.250						
0.029	—0.020	0.143	0.109	4.912					
—0.071	0.248	—0.023	0.000	—0.002	0.629				
—0.098	0.740	0.562	—0.001	0.021	0.102	0.911			
0.120	—0.172	0.526	0.291	—0.223	0.019	0.021	1.967		
0.067	—0.028	0.467	0.308	—0.268	0.022	0.055	1.459	3.126	
0.044	0.015	0.451	—0.284	—0.011	0.012	0.051	—0.005	0.044	0.668
—0.041	—0.012	—0.050	—0.003	0.149	0.015	0.034	0.009	0.014	0.017
—0.059	0.210	—0.009	0.001	0.011	—0.006	0.069	—0.098	—0.151	—0.005
—0.042	0.153	0.032	—0.007	0.016	0.015	0.076	—0.009	0.004	0.022
0.000	0.000	—0.002	0.000	0.001	0.000	0.000	0.002	—0.003	—0.001
—0.005	0.009	0.004	0.019	—0.007	—0.002	0.003	0.074	—0.022	—0.019
			0						
			0.360						
			0						
			0						
			0						
			0						

[a]Units: stretch and stretch/stretch constants in mdyn A^{-1}; stretch/bend constants in mdyn A rad^{-1}; C≡C—C—N plane.

ACKNOWLEDGEMENTS

The authors are grateful to Ragnhild Seip for recording the ED data and to Anne Horn for drawing the figures, H. P. received a postdoctoral fellowship from DEMINEX through NTNF.

REFERENCES

1 P. Klaeboe, C. J. Nielsen, H. Priebe, S. H. Schei and C. E. Sjøgren, J. Mol. Struct., 141 (1986) 161.
2 S. H. Schei, H. Priebe, C. J. Nielsen and P. Klaeboe, J. Mol. Struct., 147 (1986) 203.
3 C. J. Nielsen, P. Klaeboe, H. Priebe and S. H. Schei, J. Mol. Struct., 147 (1986) 217.
4 C. J. Nielsen and C. E. Sjøgren, J. Mol. Struct. (Theochem), 150 (1987) 361.
5 M. G. Baldwin, K. E. Johnson, J. A. Lovinger and C. O. Parker, J. Polym. Sci., Part B, 5 (1967) 803.
6 H. Priebe, Acta Chem. Scand., Part B, 38 (1984) 623.
7 H. Priebe, Acta Chem. Scand., Part B, 38 (1984) 895.

for 3-azidopropyne with reference to Fig. 8

$S_6 = \Delta\alpha_{789}$ $S_7 = \Delta\alpha_{478}$ $S_8 = \Delta\alpha_{347}$
$S_{11} = 2^{-1/2}(\Delta r_{45} - \Delta r_{46})$

$S_{20} = \Delta\phi_{234}(\parallel)$ $S_{21} = \Delta\phi_{234}(\perp)$

4.818									
0.144	0.810								
−0.025	0.077	0.647							
0.000	0.001	0.001	0.012						
−0.006	0.011	−0.004	0.002	0.028					
					5.895				
						15.780			
							0.235		
							0	0.235	
							0.129	0	0.315
							0	0.129	0	0.315

bend and bend/bend constants in mdyn Å rad^{-2}. [b] $\parallel$ $\perp$ signifies parallel and perpendicular to the

8 G. O. Braathen, P. Klaeboe, C. J. Nielsen and H. Priebe, J. Mol. Struct., 115 (1984) 197.
9 F. A. Miller and B. M. Harney, Appl. Spectrosc., 24 (1970) 291.
10 W. Zeil, J. Haase and L. Wegman, Z. Instrumentenkd., 74 (1966) 84.
11 O. Bastiansen, R. Graber and L. Wegman, Balzers High Vacuum Rep., 24 (1969) 1.
12 K. Ramagana, I. Iijima and M. Kimura, J. Mol. Struct., 30 (1976) 243.
13 B. Andersen, H. M. Seip, T. G. Strand and R. Stølevik, Acta Chem. Scand., 23 (1969) 3224.
14 S. H. Schei, Acta Chem. Scand., Part A, 37 (1983) 15.
15 T. G. Strand and R. A. Bonham, J. Chem. Phys., 40 (1964) 1686.
16 R. F. Stewart, E. R. Davidson and W. I. Simpson, J. Chem. Phys., 42 (1965) 3175.
17 K. Kuchitsu and S. J. Cyvin in S. J. Cyvin (Ed.), Molecular Structures and Vibrational Amplitudes, Elsevier, Amseterdam, 1972, Chap. 12.
18 K. Hagen and K. Hedberg, J. Am. Chem. Soc., 95 (1973) 1003.
19 J. Almlöf, The MOLECULE program system, USIP report 74-16, University of Stockholm (1974) (program manual).
20 S. Saebø, MOLFORC, University of Oslo (1980) (program manual).
21 B. Roos and P. Siegbahn, Theor. Chim. Acta, 17 (1970) 209.
22 S. Huzinaga, J. Chem. Phys., 42 (1965) 1293.
23 C. Glidewell and D. Holden, J. Mol. Struct., 89 (1982) 325.

24 E. Mantica and G. Zerbi, Gazz. Chim. Ital., 90 (1960) 53.
25 F. A. Miller and D. Bassi, Spectrochim. Acta, 19 (1963) 565.
26 C. J. Nielsen, F. M. Nicolaisen and H. Priebe, in progress.
27 J. C. Evans and R. A. Nyquist, Spectrochim. Acta, 19 (1963) 1153.
28 R. A. Nyquist, T. L. Reder, F. F. Stec and G. J. Kallos, Spectrochim. Acta, Part A, 27 (1971) 897.
29 P. Klaeboe, K. Kosa, C. J. Nielsen, H. Priebe and S. H. Schei, J. Mol. Struct., (1987) to be published.
30 C. J. Nielsen, H. Priebe, R. Salzer and S. H. Schei, J. Mol. Struct., (1987) to be published.
31 S. Bjørklund, E. Augdahl, D. H. Christensen and G. O. Sørensen, Spectrochim. Acta, Part A, 32 (1976) 1021.
32 T. Woldbaek, C. J. Nielsen and P. Klaeboe, J. Mol. Struct., 66 (1980) 31.
33 T. Woldbæk, Acta Chem. Scand., Ser. A, 36 (1982) 641.
34 P. Klaeboe, C. J. Nielsen and D. L. Powell, Spectrochim. Acta, Part A, 41 (1985) 1315.
35 K. Martinsen, D. L. Powell, C. J. Nielsen and P. Klaeboe, J. Raman Spectrosc., 17 (1986) 437.
36 P. Klaeboe, B. Klewe, K. Martinsen, C. J. Nielsen, D. L. Powell and D. J. Stubbles, J. Mol. Struct., 140 (1986) 1.
37 R. G. Jones and W. J. Orville-Thomas, J. Chem. Soc., (1965) 4635.
38 J. R. Durig and D. W. Wertz, Spectrochim. Acta, Part A, 24 (1968) 21.
39 R. D. McLachlan, Spectrochim. Acta, Part A, 23 (1967) 1793.
40 L. F. Thomas, I. E. Sherrad and J. Sheridan, Trans. Faraday Soc., 51 (1955) 619.
41 E. Hirota and Y. Morino, Bull. Chem. Soc. Jpn, 34 (1961) 341.
42 Y. Kikuchi, E. Hirota and Y. Morino, Bull. Chem. Soc. Jpn, 34 (1961) 348.
43 M. Traetteberg, P. Bakken, S. J. Cyvin, B. N. Cyvin and H. Hopf, J. Mol. Struct., 51 (1979) 77.
44 E. Gogstad, R. Stølevik and M. Traetteberg, J. Mol. Struct., 116 (1984) 295.
45 M. Traetteberg, P. Bakken, S. J. Cyvin, B. N. Cyvin and H. Hopf, J. Mol. Struct., 55 (1979) 199.
46 B. P. Winnewisser, J. Mol. Spectrosc., 82 (1980) 220.
47 D. W. Anderson, D. W. H. Rankin and A. Robertson, J. Mol. Struct., 14 (1972) 385.
48 K. O. Christe, D. Christen, H. Oberhammer and C. S. Schack, Inorg. Chem., 23 (1984) 4283.
49 A. Almenningen, B. Bak, P. Jansen and T. G. Strand, Acta Chem. Scand., 27 (1973) 1531.
50 C. George, A. H. Lowrey and J. Karle, J. Mol. Struct., 127 (1985) 107.